Inorganic Chemistry

ARTICLE

pubs.acs.org/IC

Can Human Prolidase Enzyme Use Different Metals for Full Catalytic Activity?

Marta E. Alberto, Monica Leopoldini, and Nino Russo*

Dipartimento di Chimica and Centro di Calcolo ad Alte Prestazioni per Elaborazioni Parallele e Distribuite-Centro d'Eccellenza MIUR, Universita' della Calabria, I-87030 Arcavacata di Rende (CS), Italy.

ABSTRACT: The catalytic hydrolysis of the Gly-Pro substrate by the bimetallic prolidase active site model cluster has been investigated at the DF/B3LYP level of theory, in order to provide fundamental insights into the still poorly understood mechanism of prolidase catalysis. To date, the majority of prolidases exhibits metal-dependent activity, requiring two divalent cations such as Zn^{2+}, Mn^{2+}, or Co^{2+} for maximal activity. In addition, it has been shown recently that two different metal ions in the active site of human prolidase (Zn and Mn) can coexist, with the protein remaining partially active. With the purpose of identifying which is the most efficient dimetallic center for the prolidase catalyzed reaction, Zn(II), Co(II), and Mn(II) have been examined as potential catalytic metals for this enzyme. Furthermore, to better elucidate the exact roles played by the metals occupying the site 1 and site 2 positions, the hetero-bimetallic active site having Zn and Mn cations has been also investigated, considering the two derivatives Mn1−Zn2 and Zn1−Mn2. The rate-determining step of the hydrolysis reaction is always found to be the nucleophilic addition of the hydroxide ion on the carbonyl carbon of the scissile peptide bond, followed by the less energetically demanding proline−peptide C−N bond scission. The analysis of the involved energy barriers does not indicate clearly a preference for a particular metal by the prolidase enzyme. Instead, we may point out a slightly better behavior of the cobalt-containing cluster as far as both tetrahedral formation and its decomposition are concerned, due to a greater degree of ligands-to-metals charge transfer. The mixed Mn−Zn hetero-dimetallic clusters appear to be also able to perform the hydrolysis of the Pro-Gly substrate, with a slight preference for the Mn1−Zn2 configuration.

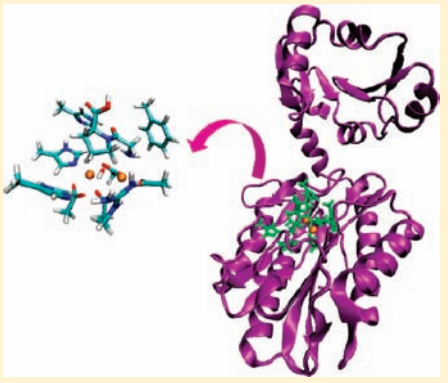

INTRODUCTION

Prolidases (EC 3.4.13.9) are metalloenzymes that catalyze the hydrolysis of the imide bond between an α-carboxyl group and a proline or hydroxyproline residue at the C-terminal end. These bonds are not susceptible to generic peptidase cleavage, since the side chain of proline may cycle back to the backbone amino group and generate a pyrrolidine ring not easy to be hydrolyzed.[1]

Only a limited number of mammalian peptidases are known to be able to hydrolyze proline adjacent bonds, and their activity is influenced by the isomeric state (cis−trans) as well as by the position of proline in the peptide chain. All the known proline-specific peptidases cleave only when the peptide bond preceding proline has trans conformation.[2,3]

Due to its peculiarity, the presence of this amino acid strongly influences the conformation, properties, and biological functions of several molecules such as peptides involved in immunomodulation and coagulation, cytokines, growth factors, and neuro- and vasoactive peptides.[3]

Members of this class have been isolated from different mammalian tissues[4] as well as from bacteria[5,6] and archea (*Pyrococcus furiosus* (*P. furiosus*)).[7]

While the physiological role of prolidase in bacteria and archaea is unclear, in humans it is relevant in the latest stage of protein catabolism particularly of those molecules rich in imino acids such as collagens, thus being involved in matrix remodeling. A deficiency of this enzyme in humans causes a recessive connective tissue disorder (prolidase deficiency) characterized by abnormalities of the skin, mental retardation, and respiratory tract infections.[8,9]

The enzyme could play also an important role in biotechnological applications. It has a potential use in the dairy industry as a cheese-ripening agent since the release of proline from peptides in cheese reduces bitterness.[10]

In addition, it was recently reported[11] that prolidase is able to hydrolyze highly toxic, organophosphorus, acetylcholinesterase inhibitors, which include various chemical warfare agents and pesticides. It has been used as target enzyme for specific melanoma prodrug activation.

Its main activity is Gly-Pro dipeptides hydrolysis,[5,12,13] although the enzyme is also active against Ala-Pro, Met-Pro, Phe-Pro, Leu-Pro, and Val-Pro. In addition, some prolidase proteins were found to be able to cleave dipeptides with proline at the N-terminal end or dipeptides that do not contain a proline residue.[13]

To date, the majority of prolidases that have been studied exhibits metal-dependent activity, requiring divalent cations such

Received: November 9, 2010
Published: March 22, 2011

ACS Publications © 2011 American Chemical Society

Scheme 1. Prolidase Proposed Catalytic Mechanism

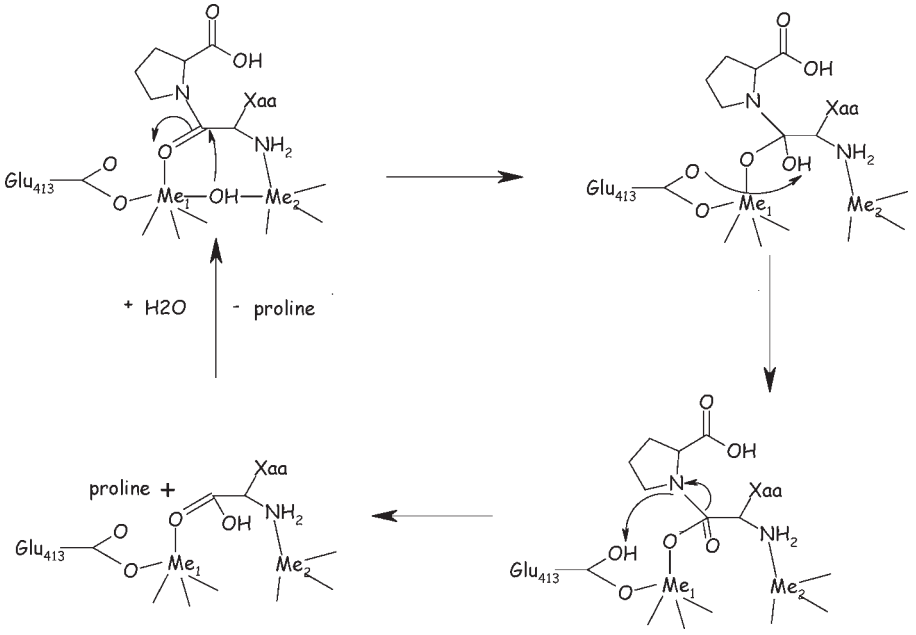

as Zn^{2+}, Mn^{2+}, or Co^{2+} for maximal activity.[14,15] They have been purified either as monomers or as dimers depending on the enzyme.[16−18]

The best characterized prolidase in terms of structure and catalytic site composition is the one isolated from the archaeon *P. furiosus* (Pfprol) for which the complete structure and active site organization have been described in detail by crystallographic and site directed mutagenesis studies, both in native and *Escherichia coli* (*E. coli*) recombinant enzyme.[19] The latter displays a 28% identity with human prolidase for which, on the contrary, information on the structure, the organization of the active site, and the catalytic mechanism are still lacking.

X-ray crystal structure analysis of *P. furiosus* cobalt-containing prolidase has identified five amino acids that function as the metal-binding residues in this enzyme. Histidine-284 and glutamate-313 solely bind to the first Co center (Co1), aspartate-209 to the second Co center (Co2), and aspartate-220 and glutamate-327 are ligands to both cobalt cations.[20,21] The corresponding residues in human prolidase are His371, Glu413, Asp277, Asp288, and Glu453.

Crystallographic works indicated that prolidase possesses five charged residues at the active site as metal ion chelating sites. All five residues were conserved among the examined prolidase protein sequences. This clearly indicates an important architecture for prolidases to maintain functionality regardless of their phylogenetic distances by evolution.[20]

Interestingly, strong structural homologies among prolidase and other proteins such as methionine aminopeptidases and proline aminopeptidase have been recognized. The dinuclear metal clusters in these enzymes are coordinated by identical sets of residues.[15] Due to these homologies, prolidase, together with methionine aminopeptidase (MetAP)[22] and proline aminopeptidase (APPro),[23] becomes a member of a group of enzymes whose most distinctive shared feature is a "pita-bread" fold of the C-terminal catalytic domain. It is suggested that they share a common reaction mechanism in which the metals coordinated hydroxide group performs a nucleophilic attack on the carbonyl carbon of the scissile peptide bond.[20] The cleavage of the amide bond is provided by a proton shift performed by a conserved Glu residue which acts as a proton shuttle, first abstracting an H^+ from the bridging nucleophile water molecule/hydroxide ion and then transferring it to the nitrogen atom of the substrate (see Scheme 1).[15] Such a role as proton carrier is similar to that proposed for Glu133 in peptide deformylase,[24] Glu270 in carboxypeptidase A,[25,26] Asp120 in β-lactamase,[27] and Glu106 in carbonic anhydrase.[28]

Like the human enzyme, Pfprol is a homodimer with two subunits. Each monomer has a dinuclear metal cluster requiring Co(II) for full activity.[20]

The enzyme activity could also be supported by the presence of Mn^{2+} as demonstrated by the results concerning the human prolidase synthesized in prokaryotic and eukaryotic hosts. The recombinant enzyme was found to require Mn(II) for full activity identical to the endogenous human fibroblasts prolidase.[29]

The effects of various bivalent ions (Ca^{2+}, Mg^{2+}, Cu^{2+}, Fe^{2+}, and Ni^{2+}) on prolidase activity were tested in several works, and the influence of the Zn(II) ions was also evaluated. *Lactobacillus delbrueckii* (*Lb. delbrueckii*) prolidase requires zinc,[16] *P. furiosus* prolidase prefers cobalt and manganese,[7] and *Lactobacillus casei* (*Lb. casei*) enzyme can utilize magnesium, manganese, and cobalt.[5] The recombinant *Lactococcus lactis* (*Lc. lactis*) prolidase showed its highest activity for Leu-Pro with zinc, but the activity with manganese was 21.5% of that with zinc. Activity was not detected with other divalent cations, i.e., cobalt, magnesium, nickel, copper, and calcium.[18] Zinc was suggested to be the essential cation to *Lactobacillus bulgaricus* (*Lb. bulgaricus*) prolidase activity.[16]

The binding site in prolidase is not highly selective about the nature of the bonded divalent ion. A typical case in this respect is represented by prolidase in *P. furiousus* (Pfprol) for which, during the crystallization process, it was observed that Zn(II)-substituted native Co(II) ions,[20] supposedly necessary for full enzymatic activity.

dx.doi.org/10.1021/ic1022517 |*Inorg. Chem.* 2011, 50, 3394–3403

In addition, the coexistence of two different metal ions in the active site of recombinant human prolidase (Zn and Mn) with the protein remaining partially active has been proven.[30] In this case, Zn(II) cation in the active site seems to lead toward a decreasing of activity although the enzyme preserves a significant efficiency.

The hetero-bimetallic center could be required for distinct functions either structural or catalytic, or alternatively, catalyzing different steps in a multistep sequence. This kind of enzymes seems to employ the two metals in different functions; thus, the positions of the individual metals are crucial in determining the catalytic efficiency.

Despite the numerous studies done to characterize prolidase structures, the identity of the in vivo metal ions for the enzyme has not been univocally established, so questions still remain regarding the exact nature of the metal centers and the roles played by the metals occupying the M1 and M2 positions. Detailed theoretical studies on the effect of metal ions on prolidases are still lacking. Thus, in an effort to identify the catalytic metal among zinc, cobalt, and manganese, we have performed a computational study on the hydrolysis of a Gly-Pro substrate by a dinuclear cluster as a model for the prolidase active site. Furthermore, we have also considered the hetero-bimetallic active site having Zn and Mn cations as the two derivatives Mn1−Zn2 and Zn1−Mn2, in order to better understand the individual roles played by the metallic center.

METHODS

The quantum mechanical (QM) studies performed on metalloenzymes use chemical models for the active sites since proteins are macromolecules not possible to be studied on the whole by ab initio QM and density functional theory (DFT) theoretical methods. Using available X-ray structures, the active site is divided into two parts, the quantum mechanical cluster and the environment, that is the portion surrounding the catalytic region not involved in catalysis.

The model for the enzyme is usually made up by the metal ion and its first coordination sphere, to which some nearby residues recognized as fundamental in catalysis are added. Ligands are represented by the functional part of the side chains only (imidazole rings for histidines, acetates for aspartates or glutamates). An atom of each amino acidic residue is usually kept frozen at its crystallographic position in order to mimic the steric effects produced by the surrounding protein and to avoid an unrealistic expansion of the cluster during the optimization procedure.[31] The environment not explicitly included in the quantum cluster has a double steric and electrostatic effect. The first one can be brutally reproduced by fixing some crystallographic positions. The electrostatic effect is introduced assuming it is a homogeneous polarizable medium with a dielectric constant usually chosen to be equal to 4.

The active site model used in this work has been built starting from the 2.45 Å X-ray structure of the recombinant human prolidase produced in *E. coli* (PDB code, 2OKN).[32] It is made up by two metallic cations (Zn, Co, and Mn) and their first coordination sphere, i.e., four CH_3COO^- groups, that mimic the Asp277, Asp288, Glu413, and Glu453, and a methylimidazole ring for the His371 amino acid. Outer sphere residues included are Phe227, His256, His378, and Arg451 modeled by methylbenzene, methylimidazole, and $[CH_3NHC(NH_2)_2]^+$, respectively. Pro-Gly dipeptide is modeled in the active site as simplest substrate, according to the binding mode of substrates of enzymes from the same family.[33]

All the computations have been carried out with the Gaussian 03 code.[34] The three-parameter hybrid exchange functional by Becke and the Lee, Yang, and Parr correlation (B3LYP) functional has been used to perform geometry optimization.[35−38] The 6-31G* basis set has been chosen for the C, N, O, P, and H atoms,[39−42] while for the metal the LANL2DZ pseudopotential in connection with the relativistic orbital basis set,[43] has been used.

Electronic ground states have been singlet for Zn-, septet for Co-, undecaplet for Mn-homo-dimetallic clusters, and sextet for the mixed Zn−Mn ones.

Geometry optimization has been followed by frequency calculations, performed on all stationary points of the reaction paths, to evaluate their character as minima or saddle points, and to compute zero point energy corrections, that have then been included in all the relative energy values.

Intrinsic reaction coordinate (IRC) calculations[44,45] have been performed with the aim to confirm that a given transition state connects a particular couple of consecutive minima.

Single-point energy calculations using the 6-311++G** basis set have been performed on the B3LYP/6-31G* optimized geometries and used to build the PESs.

The performance of the B3LYP functional in predicting properties of transition metal containing systems is supported by a large number of publications, especially concerning enzymatic catalysis[24,33,46−53] in which also hydrolysis reactions are involved.[24,33,48,50−53]

Solvent effects have been introduced as single-point computations on the optimized gas-phase structures in the framework of self-consistent reaction field polarizable continuum model (SCRF-PCM)[54−56] in which the cavity is created via a series of overlapping spheres, using the PCM approach. The united atom (UA0) topological model applied on the atomic radii of the UFF force field[57] has been used to build the cavity, in the gas-phase equilibrium geometry. The dielectric constant value $\varepsilon = 4$ has been chosen in order to take into account the coupled effect of the protein itself and the water medium surrounding the protein, according to previous suggestions.[24,33,46−53]

Natural bond orbital (NBO) analysis[58] has been carried out to determine net charges and some electronic properties.

Experience in computational enzymatic catalysis[59] suggests that an atomistic model of large dimensions is not always needed, since a great deal of the energy involves the breaking and formation of bonds and interactions in the first sphere of coordination. Long-range interactions are usually found less important. However, exceptions are not infrequent, in particular with reactions involving charge transfer. But in the cases of metallic centers, radical enzymes, enzymes lacking specific long-range interactions, or enzymes with ligands that are very small or have much localized electronic density, the increasing of the model seems that it does not bring new information to the mechanistic pathway or the energies associated with it.

RESULTS AND DISCUSSION

Zn-, Co-, and Mn-Homo-dimetallic Clusters. The optimized geometries of the stationary points belonging to the reaction sequence of Scheme 1 and referred to the homo-dimetallic clusters containing Zn, Co, and Mn dications, respectively, are presented in the Figure 1. Distances are given without parentheses for zinc, and in bracket and square parentheses for cobalt and manganese, respectively.

The complex between the enzyme active site and the substrate, ES, is obtained when the Pro-Gly substrate interacts with the Me2 metal center through the glicine amide NH_2 lone pair (Me2−N distances are 2.28, 2.23, and 2.36 Å, for zinc, cobalt, and manganese, respectively). The carbonyl oxygen of the substrate seems that it does not establish any interaction with Me1, for all considered metal species (O−Me1 distance is 4.91, 4.95, and 5.22 Å, for zinc, cobalt, and manganese, respectively). This is mainly due to the fact that the carbonyl oxygen of the

dx.doi.org/10.1021/ic1022517 |*Inorg. Chem.* 2011, 50, 3394–3403

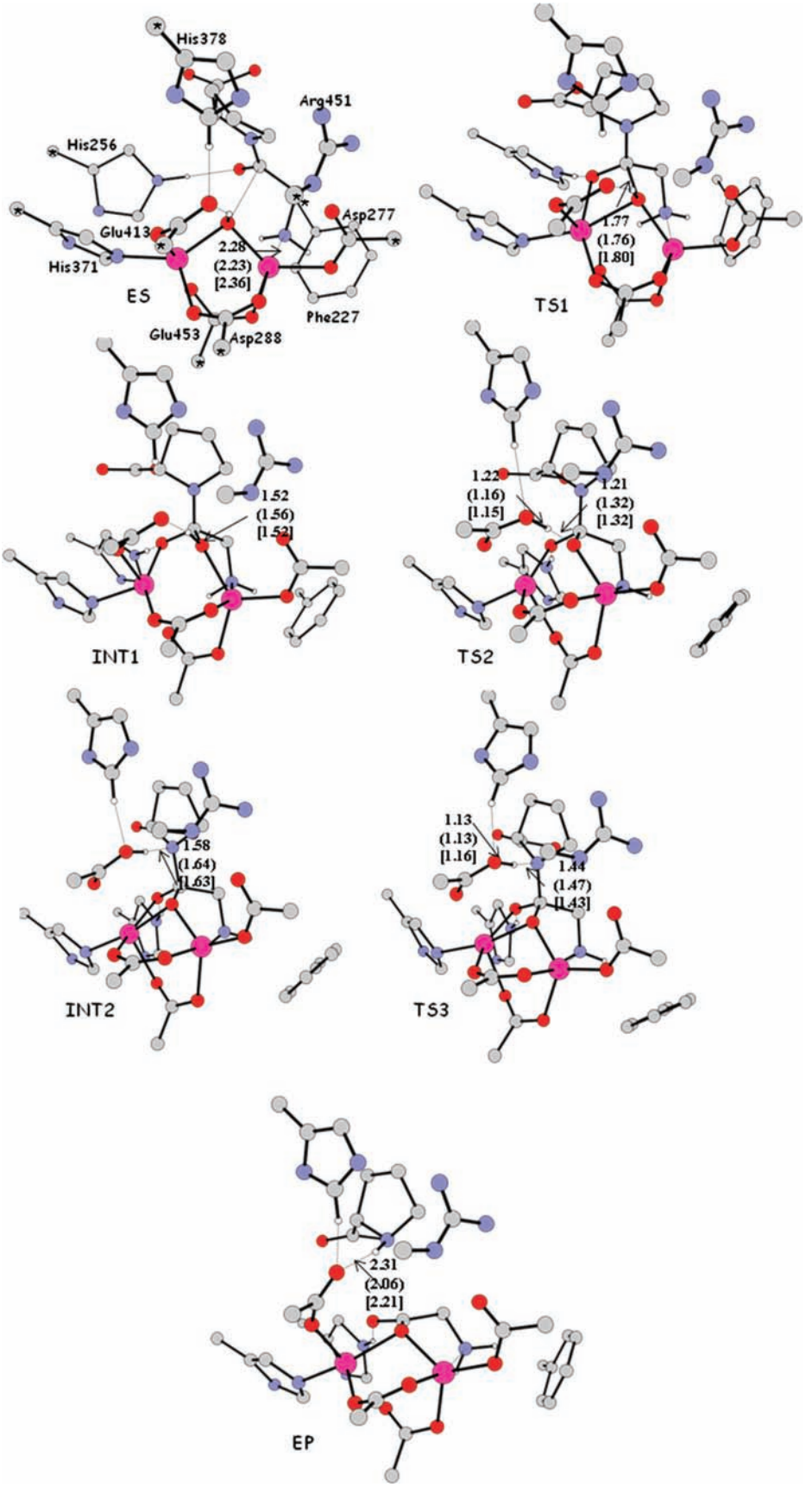

Figure 1. B3LYP optimized geometries of the points ES, TS1, INT1, TS2, INT2, TS3, and EP. Distances are given without and with bracket and square parentheses for Zn−Zn, Co−Co, and Mn−Mn clusters, respectively.

dx.doi.org/10.1021/ic1022517 |*Inorg. Chem.* 2011, 50, 3394–3403

substrate is involved in a strong H-bond with the Nδ of the His256 residue (1.88 Å for both zinc and manganese, and 1.86 Å for cobalt).

The nucleophilic attack by the bridging OH on the substrate carbon atom (TS1) occurs when the O···C distance assumes the critical value of 1.77 (zinc), 1.76 (cobalt), and 1.80 (manganese) Å. Its nature of saddle point is clearly indicated by the imaginary frequency at 179, 170, and 185 cm^{-1}, for zinc, cobalt, and manganese, respectively, whose visual inspection proposes the stretching of the $O_{OH}-C_{substrate}$ bond. The incoming negative charge of the oxygen of the C═O bond is stabilized, in addition to the H-bond with the N−H of the His256 residue, by its coordination to the Me1 center (at 2.17, 2.11, and 2.20 Å, for Zn, Co, and Mn, respectively), as can be seen from the TS1 structure reported in the Figure 1.

TS1 evolves into the tetrahedral intermediate INT1, in which the C−OH bond is completely formed at 1.52 Å for both Zn and Mn, and 1.56 Å, for Co. The OH is involved into a strong H-bond with the oxygen coming from the Glu413 residue (1.78 Å, in all three cases) that has to perform the proton shift from the OH to the intraring nitrogen of the proline, in order to be the C−N bond broken, leading to products.

First, the proton moves from the OH to the oxygen of Glu413 residue, through the transition state TS2 (imaginary frequency at 597, 525, and 444 cm^{-1}, for Zn^{2+}, Co^{2+}, and Mn^{2+}, respectively). It leads to the INT2 intermediate, in which the Glu413 is protonated and establishes a strong H-bond with the nitrogen of the proline ring, at 1.58 (Zn^{2+}), 1.64 (Co^{2+}), and 1.63 Å (Mn^{2+}). The coordination bond of Glu413 with the Me1 site is elongated from 2.13, 2.10, and 2.16 Å in the INT1 up to 2.39, 2.37, and 2.38 Å, in the INT2, for zinc, cobalt, and manganese, respectively.

Protonation of the proline nitrogen by Glu413 occurs through the transition state TS3, in which the $O_{Glu}\cdots H$ and $H-N_{proline}$ bond distances assume the values of 1.13 and 1.44 Å (zinc), 1.13 and 1.47 Å (cobalt), and 1.16 and 1.43 Å (manganese). Visual inspection of the imaginary frequency at 751, 327, and 646 cm^{-1} mainly shows the stretching of these two bonds. The C−N bond was found to be quite short (1.57 Å for zinc and manganese, and 1.56 Å for cobalt) for a transition state in which the nitrogen is being protonated, so that this TS is mainly governed by the motion of the H^+ particle.

The next step encountered on the potential energy profile after the TS3 is the final complex between products, EP. Once the intraring nitrogen of proline is protonated by Glu413 in the TS3, the cleavage of the C−N bond occurs simultaneously. In fact, all attempts to localize on the potential energy profile a stationary point characterized by a protonated proline and an intact C−N bond failed.

In the EP, the glycine was found to be bound to both the metals through one oxygen of the carboxylic group (Me1−O and Me2−O distances are 2.05 and 2.13 Å (zinc), 2.18 and 2.03 Å (cobalt), and 2.23 and 2.13 Å (manganese)) and to the Me2 site with the NH_2 (2.29, 2.30, and 2.41 Å, for zinc, cobalt, and manganese, respectively). Proline instead is hydrogen bonded to the Glu413 residue at 2.31, 2.06, and 2.21 Å, for zinc, cobalt, and manganese, respectively.

The PESs for the hydrolysis in the protein-like environment of the Pro-Gly substrate by the prolidase model cluster are reported in Figure 2, for zinc (black line), cobalt (red line), and manganese (blue line).

The energy cost (TS1) to pass from the initial ES complex to the tetrahedral intermediate INT1 is computed to be 13.1, 11.1, and 10.8 kcal/mol, for Zn^{2+}, Co^{2+}, and Mn^{2+}, respectively. These values indicate that the nucleophilic attack that seems to determine the reaction kinetics proceeds with a reasonable rate for all dications.

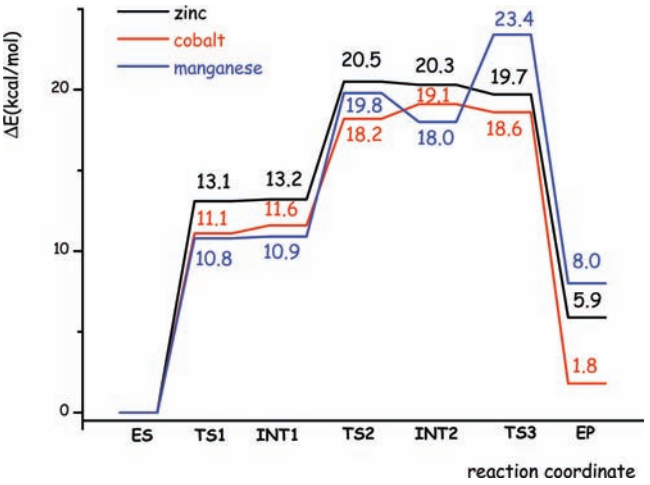

Figure 2. Potential energy surfaces in the protein like environment for the hydrolysis of Gly-Pro by prolidase, for Zn−Zn (black), Co−Co (red), and Mn−Mn (blue) clusters.

The INT1 is found to be isoenergetic with the TS1 stationary point in all examined cases, along the potential energy profile.

TS2 relative energy is 20.5, 18.2, and 19.8 kcal/mol, and therefore the energy barrier to pass from INT1 to INT2, the latter found at 20.3, 19.1, and 18.0 kcal/mol, is computed to be 7.4, 6.6, and 8.9 kcal/mol, for Zn^{2+}, Co^{2+}, and Mn^{2+}, respectively. TS3 lies at 19.7, 18.6, and 23.4 kcal/mol with respect to the ES reference, so that the last step requires a barrier of 5.4 kcal/mol in the case of manganese-containing cluster, whereas for zinc and cobalt it has a negative barrier. The slightly negative barrier predicted for zinc and cobalt clusters is mainly due to the well-known B3LYP/DFT underestimation of barriers, especially concerning H-transfer processes;[59] i.e., if the reaction barrier is very low, reactions are sometimes found to be barrierless or even have a negative barrier. This does not change our conclusions that this last step occurs very easily in the case of Zn(II) and Co(II) metals.

The final complex EP between the enzyme active site and the glycine and proline products is found at 5.9, 1.8, and 8.0 kcal/mol above the reactants ES, in the case of Zn(II), Co(II), and Mn(II), respectively. Thus, the catalyzed reaction was found to be thermoneutral in the case of cobalt cation and slightly thermodynamically unfavored for Zn^{2+} and Mn^{2+} (Figure 2).

All the examined divalent metals appear to perform well the tetrahedral intermediate formation in the hydrolysis reaction of Pro-Gly substrate. The second step in the catalyzed reaction, i.e. the protonation of the proline amide nitrogen and thus the collapse of the tetrahedral intermediate into products, seems to proceed very easily for zinc and cobalt. The manganese cluster indeed requires a certain amount of energy to perform this last step.

The analysis of the involved energy barriers for all of the studied cases within the model used does not indicate clearly a preference for a particular transition metal by the prolidase enzyme. We may point out a slightly better behavior for the cobalt-containing cluster, as suggested for *P. furiosus*, as far as both tetrahedral formation and its decomposition are concerned.

Zinc cation in the active site seems to be able to perform the Pro-Gly hydrolysis, in agreement with the observations on

dx.doi.org/10.1021/ic1022517 |*Inorg. Chem.* 2011, 50, 3394–3403

Table 1. Atomic Net Charges (in |e|) of the Stationary Points along the Potential Energy Profile of Prolidase, for Zn−Zn, Co−Co, and Mn−Mn Clusters

	ES	TS1	INT1	TS2	INT2	TS3	EP
				Mn−Mn			
O_{nuc}	−1.278	−1.072	−0.926	−1.005	−1.034	−1.023	−0.862
H_{nuc}	0.485	0.519	0.526	0.507	0.522	0.502	0.412
C_{sub}	0.722	0.768	0.753	0.750	0.747	0.752	0.826
O_{sub}	−0.710	−0.902	−0.926	−0.987	−0.992	−0.988	−0.752
N_{sub}	−0.480	−0.554	−0.587	−0.597	−0.631	−0.619	−0.707
$O1_{glu}$	−0.781	−0.796	−0.792	−0.734	−0.737	−0.740	−0.765
$O2_{glu}$	−0.848	−0.845	−0.832	−0.734	−0.703	−0.729	−0.867
Mn1	1.577	1.600	1.586	1.579	1.583	1.586	1.590
Mn2	1.576	1.573	1.574	1.572	1.571	1.578	1.579
				Zn−Zn			
O_{nuc}	−1.268	−1.044	−0.904	−0.959	−1.023	−1.015	−0.870
H_{nuc}	0.487	0.526	0.532	0.512	0.524	0.508	0.401
C_{sub}	0.729	0.771	0.756	0.754	0.749	0.753	0.825
O_{sub}	−0.715	−0.893	−0.965	0.980	−0.982	−0.978	−0.704
N_{sub}	−0.480	−0.553	−0.582	−0.591	−0.629	−0.621	−0.702
$O1_{glu}$	−0.785	−0.791	−0.787	−0.741	−0.742	−0.744	0.764
$O2_{glu}$	−0.826	−0.821	−0.811	−0.727	−0.666	−0.687	−0.852
Zn1	1.435	1.437	1.433	1.432	1.444	1.444	1.437
Zn2	1.433	1.421	1.416	1.401	1.412	1.412	1.430
				Co−Co			
O_{nuc}	−1.107	−0.948	−0.869	−0.914	−0.895	−0.891	−0.756
H_{nuc}	0.490	0.532	0.538	0.520	0.528	0.511	0.419
C_{sub}	0.729	0.779	0.768	0.763	0.757	0.762	0.834
O_{sub}	−0.714	−0.852	−0.886	−0.902	−0.915	−0.912	−0.701
N_{sub}	−0.482	−0.552	−0.576	−0.587	−0.629	−0.622	−0.726
$O1_{glu}$	−0.775	−0.789	−0.784	−0.738	−0.743	−0.748	−0.758
$O2_{glu}$	−0.782	−0.770	−0.763	−0.666	−0.637	−0.657	−0.770
Co1	1.141	1.141	1.143	1.134	1.145	1.146	1.160
Co2	1.156	1.120	1.111	1.090	1.121	1.122	1.127

Lc. lactis[18,61] and *Lb. delbrueckii*[16,62] enzymes, requiring zinc for full catalytic activity.

It must be underlined here that the active site in all experimentally examined prolidases is made up by the same residues, in spite of the particular metal enclosed. At this time, it is unclear to what degree the metal ions used in vivo are intrinsic to the individual enzymes or are determined by ambient levels of ions within the organism and/or cloning, expression, and growth conditions.

In the Table 1, the natural charges obtained through NBO analysis are collected for all the stationary points encountered on the potential energy profiles of the Zn-, Co-, and Mn-containing clusters.

The natural charges exhibited by the metals in all seven stationary points indicate that, in the case of cobalt, a certain charge transfer from ligands to cation seems to occur. For example, in the Co−ES species, natural charges on sites 1 and 2 are 1.141 and 1.156 |*e*|. The charge transfer seems to occur mainly from the bridging OH (−1.107 |*e*|) and from the oxygen atom of the Glu413 residue, directly coordinated to the Co1 (−0.782 |*e*|). This charge distribution is retained from the beginning to the end of the reaction (see Table 1).

In the Zn- and Mn-containing clusters, this behavior is less pronounced. By taking again the first species encountered as reference, the charges on Zn1 and Zn2, and Mn1 and Mn2 are 1.435 and 1.433 |*e*|, and 1.577 and 1.576 |*e*|, respectively. This situation results in a natural charge on the oxygen atoms of the OH and of the Glu413 ligands of −1.268 and −0.826 |*e*|, and −1.278 and −0.848 |*e*|, in the case of Zn^{2+} and Mn^{2+}, respectively. Ligands-to-metals charge transfer seems to be responsible for the slightly better performance of the cobalt cation as compared to zinc and manganese ions.

The results support the reaction mechanism reported in the Scheme 1, involving the OH attack on substrate and the protonation of amide nitrogen by the Glu/Asp residue, usually established for the metallohydrolases class of enzymes. However, prolidase seems to be to some extent different from the other peptidases, as far as the decomposition of the tetrahedral intermediate is concerned. In fact, most of the computational studies[24,33,51,52] have generally predicted a single-step reaction path for the reactions catalyzed by these enzymes; that is, once the nucleophilic addition takes place, the collapse into products occurs very easily without further energy cost. This has been found for peptide deformylase,[24] methionine aminopeptidase,[33] thermolysin,[60] and insulin-degrading enzyme (IDE).[52] The presence of the five-membered pyrrolidine ring causes a lesser reactivity of the amide nitrogen toward protonation, as well as a steric effect on the interaction of the substrate with the enzyme, leading to a relatively low amount of energy for the tetrahedral intermediate decomposition, through the proton shift performed by the glutamate residue.

Zn−Mn Hetero-dimetallic Clusters. A recent study on recombinant human prolidase produced in *E. coli*[30] has established the first experimental corroboration that two different kinds of metals, Mn and Zn, can be simultaneously present in the active site, with the protein maintaining its catalytic activity.

Actually, there is also some evidence that in prolidase the binding site is not highly selective about the nature of the bonded divalent ion. A typical case in this respect is prolidase from *P. furiousus* wherein the crystal Zn(II) substitutes Co(II), supposedly necessary for full enzymatic activity.[20] Even in the presence of overconcentrated Zn(II) ions, the protein partially retains its enzymatic activity if at least one out of the four metal binding sites in the dimeric protein is occupied by a Mn(II) ion.[30]

The optimized geometries of the stationary points belonging to the reaction sequence of Scheme 1 and referred to the hetero-dimetallic clusters containing Zn and Mn dications at both sites 1 and 2 are presented in the Figure 3. The two clusters are indicated as Zn1−Mn2 and Mn1−Zn2, depending on the occurrence of the metal at site 1, characterized by the His ligand, and site 2. Distances are given without and with parentheses, for Mn1−Zn2 and Zn1−Mn2 clusters, respectively.

The substrate approaches the active site through glycine NH_2 coordination to Me2 (at 2.27 and 2.36 Å, for the Mn1−Zn2 and Zn1−Mn2 clusters, respectively). No interaction is found between the substrate carbonyl oxygen and the Me1 (distances are 4.88 (Mn1−Zn2) and 5.12 Å (Zn1−Mn2)), the oxygen being involved in a strong H-bond with Nδ of the His256 amino acid (see Figure 3). The O_{OH} and $C_{substrate}$ distances take the values of 3.27 and 3.38 Å, whereas the bridging OH is hydrogen bonded to the Glu413 at 2.25 and 2.18 Å, as far as the Mn1−Zn2 and Zn1−Mn2 clusters are concerned. Both metals appear to be five-coordinated in both the two configurations.

The optimized transition state (TS1) structures for nucleophilic attack by the OH shows a critical distance for the O···C

dx.doi.org/10.1021/ic1022517 |*Inorg. Chem.* 2011, 50, 3394–3403

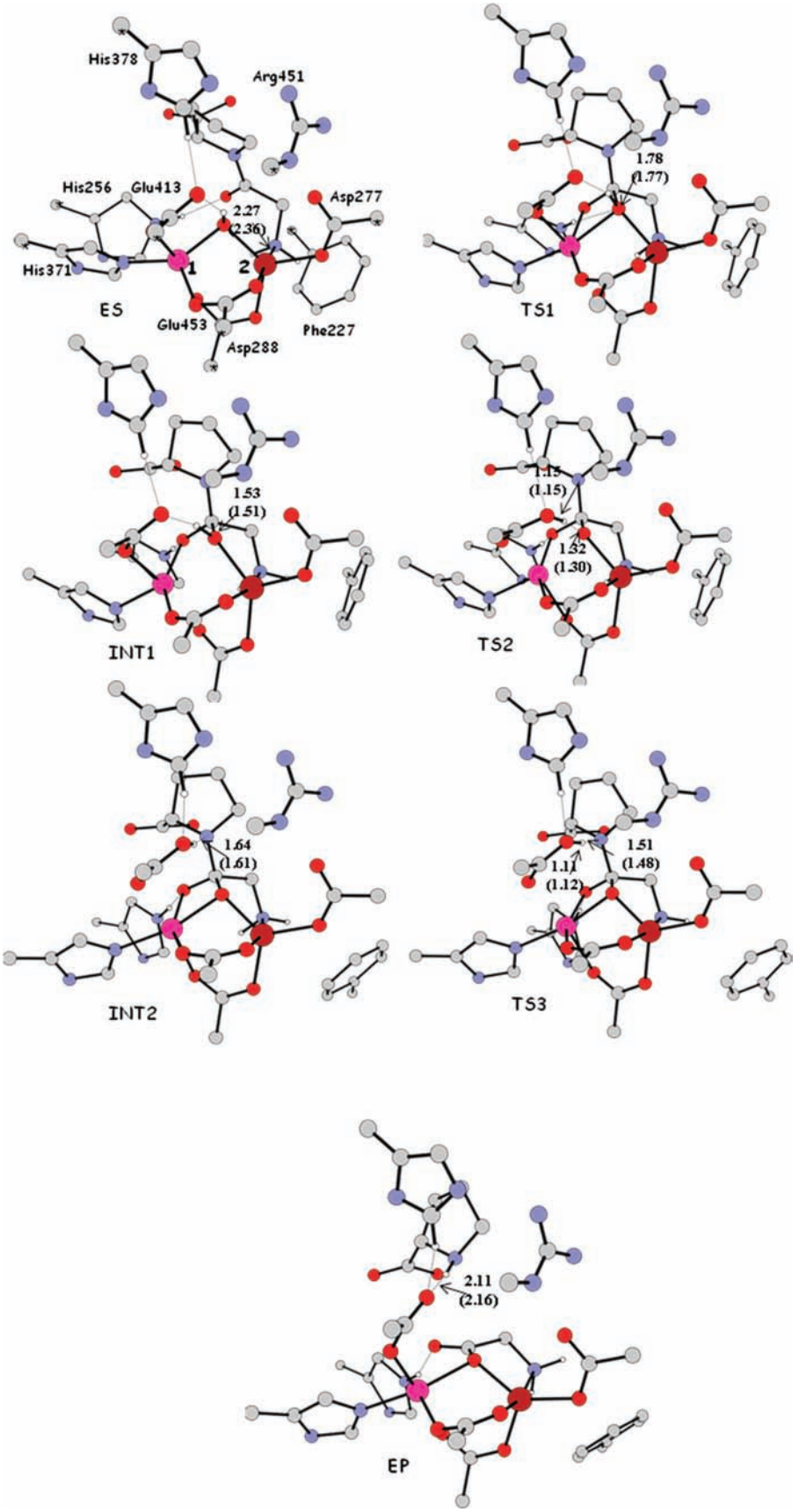

Figure 3. B3LYP optimized geometries of the points ES, TS1, INT1, TS2, INT2, TS3, and EP. Distances are given without and with parentheses, for Mn1−Zn2 and Zn1−Mn2 clusters, respectively.

dx.doi.org/10.1021/ic1022517 |*Inorg. Chem.* 2011, 50, 3394–3403

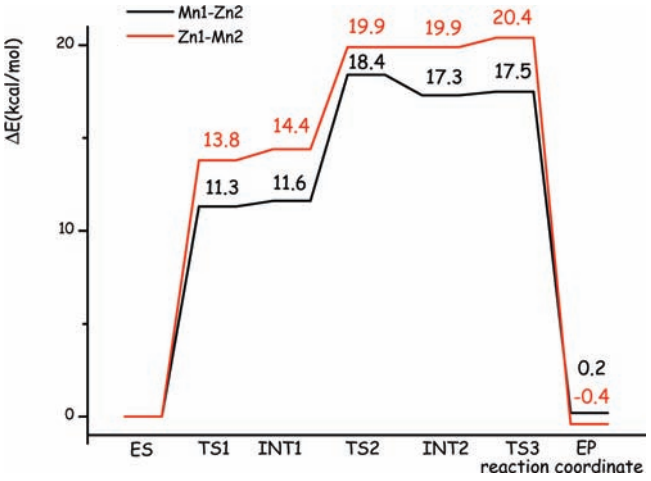

Figure 4. Potential energy surfaces in the protein-like environment for the hydrolysis of Gly-Pro by prolidase, for Mn1−Zn2 (black), and Zn1−Mn2 (red) clusters.

bond of 1.78 and 1.77 Å, for the Mn1−Zn2 and Zn1−Mn2 clusters, respectively. The substrate carbonyl oxygen interacts with site 1 at 2.20 (Mn1−Zn2) and 2.17 Å (Zn1−Mn2). It receives a H-bond from His256, of 1.75 Å length in both cases. Hessian calculations show one imaginary frequency at 181 and 182 cm^{-1}, for the Mn1−Zn2 and Zn1−Mn2, respectively, and it corresponds to the reaction coordinate describing the C−O bond formation.

After the TS1, the tetrahedral intermediate INT1 originates. It shows a $C-O_{OH}$ σ bond of 1.53 and 1.51 Å, a O···Me1 coordination bond of 2.10 and 2.04 Å, and a H-bonding interaction between the Glu413 and the bridging OH of 1.79 and 1.77 Å, in the case of the Mn1−Zn2 and Zn1−Mn2, in the order. The hydroxyl group is now not a ligand at site 1 (distances are 2.53 and 2.61 Å), whereas it is retained at site 2 in both cases.

The OH group is being deprotonated through the transition state TS2, characterized by an imaginary frequency at 375 and 436 cm^{-1} corresponding to the normal mode associated with the H^+ shift from the OH to the oxygen of the Glu413 residue.

A neutral Glu413 is found in the next optimized intermediate INT2. The oxygen of the initial OH is again bridging the two metals because of its increased negative charge, at 2.17 and 2.04 Å, and at 2.10 and 2.06 Å, for sites 1 and 2, as far as the two Mn1−Zn2 and Zn1−Mn2 clusters are involved. Proline nitrogen with an approximately sp^3 hybridization is interacting with the Glu413 through a H-bond whose length is found to be 1.64 (Mn1−Zn2) and 1.61 Å (Zn1−Mn2).

Through the transition state TS3 (imaginary frequency at 192 and 283 cm^{-1}) protonation of the proline nitrogen occurs. Visual inspection of the vibrational normal mode provides the stretching of the O_{Glu}···H and H···N_{pro} couple of bonds, whose critical distances are 1.11 and 1.51 Å, and 1.12 and 1.48 Å, respectively, as far as the Mn1−Zn2 and Zn1−Mn2 configurations are concerned. As occurred in the case of the homometallic cluster, the C−N bond in the substrate is quite short (1.56 Å in both cases), indicating again that this saddle point is mainly governed by the proton shift rather than by the C−N bond rupture.

Finally, the complex between products, EP, is identified along the reaction profile. Glycine is bound at the active site with the NH_2 group at site 2, at 2.35 Å in both cases, and with the carboxylic oxygen at both sites (Me1···O and Me2···O distances are 2.20 and 2.07 Å, and 2.08 and 2.28 Å, for the Mn1−Zn2 and Zn1−Mn2, respectively). Proline remains in the active site by establishing a hydrogen bonding interaction with Glu413 at 2.11 (Mn1−Zn2) and 2.16 Å (Zn1−Mn2).

Table 2. Atomic Net Charges (in |e|) of the Stationary Points along the Potential Energy Profile of Prolidase, for Mn1−Zn2 and Zn1−Mn2 Clusters

	ES	TS1	INT1	TS2	INT2	TS3	EP
			Mn1−Zn2				
O_{nuc}	−1.210	−1.020	−0.893	−0.972	−0.988	−0.983	−0.820
H_{nuc}	0.490	0.526	0.533	0.515	0.530	0.516	0.417
C_{sub}	0.728	0.775	0.762	0.759	0.750	0.755	0.825
O_{sub}	−0.714	−0.862	−0.920	−0.935	−0.945	−0.943	−0.710
N_{sub}	−0.481	−0.552	−0.582	−0.590	−0.628	−0.623	−0.720
$O1_{glu}$	−0.784	−0.793	−0.790	−0.731	−0.742	−0.743	−0.762
$O2_{glu}$	0.794	−0.784	−0.775	−0.686	−0.649	−0.666	−0.796
Mn1	1.428	1.433	1.432	1.428	1.440	1.440	1.435
Zn2	1.268	1.233	1.225	1.205	1.227	1.228	1.252
			Zn1−Mn2				
O_{nuc}	−1.323	−1.081	−0.924	−1.024	−1.065	−1.062	−0.871
H_{nuc}	0.482	0.521	0.525	0.509	0.520	0.508	0.362
C_{sub}	0.725	0.764	0.748	0.745	0.743	0.746	0.824
O_{sub}	−0.714	−0.928	−1.010	−1.022	−1.013	−1.013	−0.776
N_{sub}	−0.480	−0.558	−0.588	−0.595	−0.632	−0.628	−0.704
$O1_{glu}$	−0.784	−0.797	−0.588	−0.742	−0.740	−0.744	−0.745
$O2_{glu}$	−0.879	−0.866	−0.856	−0.744	−0.708	−0.728	−0.924
Zn1	1.752	1.744	1.738	1.732	1.727	1.736	1.747
Mn2	1.569	1.570	1.570	1.569	1.567	1.582	1.585

The PES in the protein-like environment for the Mn1−Zn2 and Zn1−Mn2 clusters are illustrated in the Figure 4, as black and red lines, respectively.

The nucleophilic attack occurs with a very feasible energy barrier, of 11.3 and 13.8 kcal/mol, and it leads to the intermediate INT1 lying at 11.6 and 14.4 kcal/mol, as far as Mn1−Zn2 and Zn1−Mn2 clusters are concerned. The TS2 relative energy is computed to be 18.4 and 19.9 kcal/mol, so that an energy cost of 6.8 and 5.5 kcal/mol (computed with respect to the INT1 species), for the Mn1−Zn2 and Zn1−Mn2 clusters, respectively, is required. INT2 is found at 17.3 (Mn1−Zn2) and 19.9 kcal/mol (Zn1−Mn2) along the PES. The last transition state TS3 relative energy is 17.5 and 20.4 kcal/mol, so that INT2 → TS3 conversion seems to occur very easily. The products EP are isoenergetic with respect to the reference ES (−0.4 and +0.2 kcal/mol), so the reaction appears to be again quite thermoneutral.

The overall energy diagrams show some differences in energetics between the models. Particularly, the Zn1−Mn2 potential energy profile lies slightly over the one of the Mn1−Zn2 cluster. A look at the natural charges of the stationary points, reported in the Table 2, indicates again a correlation between the better performance and the charge transfer from ligands to metals, occurring in the Mn1−Zn2 cluster rather than in the Zn1−Mn2 one. Mn when it is present at site 1 exhibits an average natural charge of ≈1.434 |e|, whereas Zn at site 2 has a natural charge of ≈1.234 |e|. Ligands responsible for this charge transfer are the nucleophile OH and the site 1 coordinated Glu413 oxygen atom. In the case of the Zn1−Mn2 cluster, indeed, the charges exhibited by

dx.doi.org/10.1021/ic1022517 |Inorg. Chem. 2011, 50, 3394–3403

the two metals are, as average values, 1.739 and 1.573 |*e*| at sites 1 and 2, respectively.

Mn and Zn substitution reveals the role of the metal positions in the catalysis. Site 1 seems to be involved in the first step of the reaction, that is the nucleophilic addition on the substrate carbonyl carbon, since Mn → Zn substitution at this position entails an increase in the energy barrier of 2.5 kcal/mol and also a destabilization of the INT1 by 2.8 kcal/mol. Site 2 indeed is implicated in the collapse of the tetrahedral intermediate into the products. In fact, Zn → Mn replacement entails slightly higher energies in this step of the reaction.

The PESs obtained with the hetero-dimetallic clusters are also very feasible. The contemporaneous presence of Mn and Zn at the active site at both sites in fact gives two clusters that are able to perform the hydrolysis of the Pro-Gly substrate, with a slight preference for the Mn1−Zn2 configuration.

CONCLUSIONS

In this paper, the catalytic mechanism of the prolidase, a bimetallic enzyme involved in the hydrolysis of iminodipeptides containing a proline or hydroxyproline residue at the C-terminal end, has been investigated through DFT methods.

The model cluster used to simulate the active site of the enzyme, made up by 120 atoms, has been large enough to reliably reproduce the hydrolysis of the Pro-Gly model for the substrate.

Three metal cations, Zn, Co, and Mn, have been examined as probable catalytically active cations.

The simultaneous presence of two different kinds of metals (Mn and Zn) in the active site has also been examined.

On the basis of the obtained results, we can summarize the following conclusions.

Independently of the particular divalent metal, the hydrolysis reaction is made up by two steps, the nucleophilic addition by the metals-bridging hydroxide ion on the peptide carbonyl carbon atom and leading to a tetrahedral intermediate. Protonation of the proline nitrogen in this intermediate, performed by the Glu413 residue, entails the release of the two products, glycine and proline.

The rate-determining step may be always identified in the nucleophilic attack step. The protonation step seems to require lower energies in all examined cases.

The proposed role of the Glu413 amino acid in the active site as a proton shuttle is also confirmed.

The obtained potential energy profiles for the homo-dimetallic clusters containing zinc, cobalt, and manganese seem to be very feasible in all three cases, with very small differences in energetics. A clear dependence of the catalytic activity on a particular transition metal is not revealed. These findings are in agreement with the experimental suggestions, indicating zinc as the likely catalytic ion for enzyme from lactic acid bacteria but indicating cobalt in the case of *P. furiosus* prolidase.

A slightly better performance of the cobalt-containing cluster appears to be associated with the occurrence of a charge transfer from ligands to metals, not observed for zinc and manganese divalent metals.

The simultaneous presence in the active site of two different kinds of metals, Mn and Zn, reveals the role of the metal positions in the catalysis. Site 1 seems to be involved in the first step of the reaction, that is, the nucleophilic addition on the substrate carbonyl carbon, since Mn → Zn substitution at this position entails a slight increase in the energy barrier. Site 2 indeed is implicated in the collapse of the tetrahedral intermediate into the products, since Zn → Mn replacement entails slightly higher energies in this step of the reaction. However, also these clusters are able to perform the hydrolysis of the Pro-Gly substrate, with a slight preference for the occurrence of Mn at site 1 and Zn at site 2.

The results obtained in this study reveal that the active site does not determine the dependence of the catalytic activity on the bonded divalent ion. Preferential selections on metallic ions in prolidases are probably matters related to specific Xaa-Pro substrates they utilize in vivo or to particular interactions in some region of the protein not included in our computations.

AUTHOR INFORMATION

Corresponding Author
*E-mail: nrusso@unical.it.

ACKNOWLEDGMENT

The University of Calabria and MIUR (Grant PRIN 2008F5A3AF_005) are gratefully acknowledged for financial support.

REFERENCES

(1) Myara, I.; Charpentier, C.; Lemonnier, A. *Life Sci.* **1984**, *34*, 1985–1998.
(2) Vanhoof, G.; Goossens, F.; De Meester, I.; Hendriks, D.; Scharpe, S. *FASEB J.* **1995**, *9*, 736–744.
(3) Yaron, A.; Naider, F. *Crit. Rev. Biochem. Mol. Biol.* **1993**, *28*, 31–81.
(4) *Connective tissue and its heritable disorders*. Royce, P. M., Steinmann, B., Eds.; Wiley-Liss: New York, 2002; pp 727−743.
(5) Fernandez-Espla, M. D.; Martin-Hernandez, M. C.; Fox, P. F. *Appl. Environ. Microbiol.* **1997**, *63*, 314–316.
(6) Suga, K.; Kabashima, T.; Ito, K.; Tsuru, D.; Okamura, H.; Kataoka, J.; Yoshimoto, T. *Biosci. Biotechnol. Biochem.* **1995**, *59*, 2087–2090.
(7) Ghosh, M.; Grunden, A. M.; Dunn, D. M.; Weiss, R.; Adams, M. W. *J. Bacteriol.* **1998**, *180*, 4781–4789.
(8) Forlino, A.; Lupi, A.; Vaghi, P.; Icaro Cornaglia, A.; Calligaro, A.; Campari, E.; Cetta, G. *Hum. Genet.* **2002**, *111*, 314–22.
(9) Endo, F.; Tanoue, A.; Hata, A.; Kitano, A.; Matsuda, I. *J. Inherited Metab. Dis.* **1989**, *12*, 351–354.
(10) Bockelmann, W. *Int. Dairy J.* **1995**, *5*, 977–994.
(11) Cheng, T. C.; Harvey, S. P.; Chen, G. L. *Appl. Environ. Microbiol.* **1996**, *62*, 1636–1641.
(12) Browne, P.; O'Cuinn, G. *J. Biol. Chem.* **1983**, *258*, 6147–6154.
(13) Fujii, M.; Nagaoka, Y.; Imamura, S.; Shimizu, T. *Biosci. Biotechnol. Biochem.* **1996**, *60*, 1118–1122.
(14) Wilcox, D. E. *Chem. Rev.* **1996**, *96*, 2435–2458.
(15) Lowther, W. T.; Matthews, B. W. *Chem. Rev.* **2002**, *102*, 4581–4608.
(16) Morel, F.; Frot-Coutaz, J.; Aubel, D.; Portalier, R.; Atlan, D. *Microbiology* **1999**, *145*, 437–446.
(17) Kobayashi, M.; Shimizu, S. *Eur. J. Biochem.* **1999**, *261*, 1–9.
(18) Yang, S. I.; Tanaka, T. *FEBS J.* **2008**, *275*, 271–280.
(19) Du, X.; Tove, S.; Kast-Hutcheson, K.; Grunden, A. M. *FEBS Lett.* **2005**, *579*, 6140–6146.
(20) Maher, M. J.; Ghosh, M.; Grunden, A. M.; Menon, A. L.; Adams, M. W.; Freeman, H. C.; Guss, J. M. *Biochemistry* **2004**, *43*, 2771–2783.
(21) Willingham, K.; Maher, M. J.; Grunden, A. M.; Ghosh, M.; Adams, M. W.; Freeman, H. C.; Guss, J. M. *Acta Crystallogr., Sect. D: Biol. Crystallogr.* **2001**, *57*, 428–430.

(22) Roderick, S. L.; Matthews, B. W. *Biochemistry* **1993**, *32*, 3907–3912.
(23) Wilce, M. C. J.; Bond, C. S.; Dixon, N. E.; Freeman, H. C.; Guss, J. M.; Lilley, P. E.; Wilce, J. A. *Proc. Natl. Acad. Sci. U.S.A.* **1998**, *95*, 3472–3477.
(24) Leopoldini, M.; Russo, N.; Toscano, M. *J. Phys. Chem. B* **2006**, *110*, 1063–1072.
(25) Abashkin, Y. G.; Burt, S. K. ; Collins, J. R. ; Cachau, R. E. ; Russo, N. ; Erickson, J. W. In *Metal-Ligand Interactions: Structure and Reactivity*; Russo, N., Salahub, D. R., Eds.; Nato Science Series 474; Kluwer: Dordrecht, The Netherlands, 1996; pp 1−22.
(26) Bertini, I.; Luchinat, C. In *Bioinorganic Chemistry*; Bertini, I., Gray, H. B., Lippard, S. J., Valentine, J. S., Eds.; University Science Books: Mill Valley, CA, 1994.
(27) Olsen, L.; Anthony, J.; Ryde, U.; Adolph, H. W.; Hemmingsen, L. *J. Phys. Chem. B* **2003**, *107*, 2366–2375.
(28) Marino, T.; Russo, N.; Toscano, M. *J. Am. Chem. Soc.* **2005**, *127*, 4242–4253.
(29) Lupi, A.; Tenni, R.; Rossi, A.; Cetta, G.; Forlino, A. *Amino Acids* **2008**, *35*, 739–752.
(30) Besio, R.; Alleva, S.; Forlino, A.; Lupi, A.; Meneghini, C.; Minicozzi, V.; Profumo, A.; Stellato, F.; Tenni, R.; Morante, S. *Eur. Biophys. J.* **2009**, in press (DOI: 10.1007/s00249-009-0459-4).
(31) Siegbahn, P. E. M.; Blomberg, M. R. A. *Chem. Rev.* **2000**, *100*, 421–437.
(32) Mueller, U., Niesen, F. H., Roske, Y., Goetx, F., Behlke, J., Buessow, K., Heinemann, U. 2007, submitted for publication (DOI:10.2210/pdb2okn/pdb).
(33) Leopoldini, M.; Russo, N.; Toscano, M. *J. Am. Chem. Soc.* **2007**, *129*, 7776–7784.
(34) Frisch, M. J.; Trucks, G. W.; Schlegel, H. B.; Scuseria, G. E.; Robb, M. A.; Cheeseman, J. R.; Montgomery, J. A., Jr.; Vreven, T.; Kudin, K. N.; Burant, J. C.; Millam, J. M.; Iyengar, S. S.; Tomasi, J.; Barone, V.; Mennucci, B.; Cossi, M.; Scalmani, G.; Rega, N.; Petersson, G. A.; Nakatsuji, H.; Hada, M.; Ehara, M.; Toyota, K.; Fukuda, R.; Hasegawa, J.; Ishida, M.; Nakajima, T.; Honda, Y.; Kitao, O.; Nakai, H.; Klene, M.; Li, X.; Knox, J. E.; Hratchian, H. P.; Cross, J. B.; Bakken, V.; Adamo, C.; Jaramillo, J.; Gomperts, R.; Stratmann, R. E.; Yazyev, O.; Austin, A. J.; Cammi, R.; Pomelli, C.; Ochterski, J. W.; Ayala, P. Y.; Morokuma, K.; Voth, G. A.; Salvador, P.; Dannenberg, J. J.; Zakrzewski, V. G.; Dapprich, S.; Daniels, A. D.; Strain, M. C.; Farkas, O.; Malick, D. K.; Rabuck, A. D.; Raghavachari, K.; Foresman, J. B.; Ortiz, J. V.; Cui, Q.; Baboul, A. G.; Clifford, S.; Cioslowski, J.; Stefanov, B. B.; Liu, G.; Liashenko, A.; Piskorz, P.; Komaromi, I.; Martin, R. L.; Fox, D. J.; Keith, T.; Al-Laham, M. A.; Peng, C. Y.; Nanayakkara, A.; Challacombe, M.; Gill, P. M. W.; Johnson, B.; Chen, W.; Wong, M. W.; Gonzalez, C.; and Pople, J. A. *Gaussian 03*, Revision C.02; Gaussian: Wallingford, CT, 2004.
(35) Becke, A. D. *J. Chem. Phys.* **1993**, *98*, 5648–5652.
(36) Lee, C.; Yang, W.; Parr, R. G. *Phys. Rev. B* **1988**, *37*, 785–789.
(37) Becke, A. D. *J. Chem. Phys.* **1993**, *98*, 1372–1377.
(38) Becke, A. D. *Phys. Rev. A* **1988**, *38*, 3098–3100.
(39) Ditchfield, R.; Hehre, W. J.; Pople, J. A. *J. Chem. Phys.* **1971**, *54*, 724–728.
(40) Hehre, W. J.; Ditchfield, R.; Pople, J. A. *J. Chem. Phys.* **1972**, *56*, 2257–2262.
(41) Hariharan, P. C.; Pople, J. A. *Mol. Phys.* **1974**, *27*, 209–214.
(42) Gordon, M. S. *Chem. Phys. Lett.* **1980**, *76*, 163–168.
(43) Dolg, M.; Wedig, U.; Stoll, H.; Preuss, H *J. Chem. Phys.* **1987**, *86*, 866–872.
(44) Gonzalez, C.; Schlegel, H. B. *J. Chem. Phys.* **1989**, *90*, 2154–2161.
(45) Gonzalez, C.; Schlegel, H. B. *J. Phys. Chem.* **1990**, *94*, 5523–5527.
(46) Leopoldini, M.; Russo, N.; Toscano, M.; Dulak, M.; Wesoloski, A. T. *Chem.—Eur. J.* **2006**, *12*, 2532–2541.
(47) Leopoldini, M.; Russo, N.; Toscano, M. *Chem.—Eur. J.* **2007**, *13*, 2109–2117.
(48) Leopoldini, M.; Marino, T.; Russo, N.; Toscano, M. *Int. J. Quantum Chem.* **2008**, *108*, 2023–2029.
(49) Leopoldini, M.; Chiodo, S. G.; Toscano, M.; Russo, N. *Chem.—Eur. J.* **2008**, *14*, 8674–8681.
(50) Leopoldini, M.; Marino, T.; Toscano, M. *Theor. Chem. Acc.* **2008**, *120*, 459–466.
(51) Leopoldini, M.; Russo, N.; Toscano, M. *Chem.—Eur. J.* **2009**, *15*, 8674–8681.
(52) Amata, O.; Marino, T.; Russo, N.; Toscano, M. *J. Am. Chem. Soc.* **2009**, *131*, 14804–14811.
(53) Alberto, M. E.; Marino, T.; Ramos, M. J.; Russo, N. *J. Chem. Theory Comput.* **2010**, *6*, 2424–2433.
(54) Miertus, S.; Scrocco, E.; Tomasi, J. *Chem. Phys.* **1981**, *55*, 117–129.
(55) Miertus, S.; Tomasi, J. *Chem. Phys.* **1982**, *65*, 239–245.
(56) Cossi, M.; Barone, V.; Commi, R.; Tomasi, J. *Chem. Phys. Lett.* **1996**, *255*, 327–335.
(57) Barone, V.; Cossi, M.; Menucci, B.; Tomasi, J. *J. Chem. Phys.* **1997**, *107*, 3210–3221.
(58) Glendening; E. D.; Reed, A. E.; Carpenter, J. E.; Weinhold, F. *NBO*, version 3.1; University of Wisconsin: Madison, WI
(59) Ramos, M. J.; Fernandes, P. A. *Acc. Chem. Res.* **2008**, *41*, 689–698.
(60) Pelmenschikov, V.; Blomberg, M. R. A.; Siegbahn, P. E. M. *J. Biol. Inorg. Chem.* **2002**, *7*, 284–298.
(61) Booth, M.; Jennings, V.; Fhaolain, I. N.; Ocuinn, G. *J. Dairy Res.* **1990**, *57*, 245–254.
(62) Gilbert, C.; Atlan, D.; Blanc, B.; Portalier, R. *Microbiology* **1994**, *140*, 537–542.